

SOUND RADIATION AND SOUND INSULATION PERFORMANCES OF MARITIME BULKHEADS

Edoardo A. Piana

Department of Mechanical and Industrial Engineering, University of Brescia, Italy
email: edoardo.piana@unibs.it

Ulf Carlsson and Leping Feng

Department of Aeronautical and Vehicle Engineering, Royal Institute of Technology (KTH), Stockholm, Sweden

Massimo Guzzo

Intermarine S.p.A., Sarzana, Italy

The research of materials matching low weight and high resistance has always been a key factor in the shipbuilding industry to increase performances and loading capacity. Nowadays, other issues add up to economical convenience, and building quiet ships is important not only for passengers and cabin crew, but also to make harbor areas more comfortable and to respect the aquatic environment. In this context, using sandwich or composite materials must be carefully evaluated and the sound insulation performances must be considered throughout all stages of the design process. This work presents some evaluations about the sound insulation performances of a ribbed fiberglass bulkhead and of a balsa-core sandwich bulkhead. In particular, the bending stiffness and the sound transmission loss obtained by sound transmission suites and mobility measurements are provided. From such measurements it has also been possible to determine the radiation efficiency of the structures, whose optimization is particularly important when a reduction of the noise pollution is required.

Keywords: bending stiffness, wave propagation, coincidence frequency, sound transmission loss, sound radiation efficiency

1. Introduction

The application of sandwich and ribbed structures is widespread in the transportation industry, where they are often preferred to traditional materials for their low weight and high loading capacity. However, these are not the sole characteristics that the structures must possess. For example, in the shipbuilding industry not only is the comfort of cabin crew and passengers regulated by noise and vibration guidelines [1], but also the noise from ships when they are operating in ports is becoming a growing concern, due to the will of planning denser and denser towns and to convert harbor districts into lively housing areas [2] and to a considerable modeling complexity [3]. Being able to predict and optimize the vibro-acoustic performances of non conventional materials is therefore of great importance. It was shown that from the frequency-dependent “apparent” bending stiffness of a composite structure, determined on the basis of a

sixth-order differential equation, it is possible to satisfactorily predict its sound transmission loss STL [4] and the radiation efficiency. The apparent bending stiffness can be evaluated analytically or by means of measurements carried out on beams or on plates. The STL of sandwich structures can be predicted using Cremer's model for homogeneous panels by using the apparent bending stiffness function instead of a constant bending stiffness value. An analogous method can be used to predict the sound radiation efficiency of maritime structures by applying a frequency-dependent bending stiffness to Leppington's theory. In this work, the STL and sound radiation ratio of a ribbed fiberglass bulkhead and of a balsa-core sandwich bulkhead computed according to this model are presented, and a comparison to measurements in sound transmission suites is provided.

2. Vibro-acoustic properties of partitions

Partitions are often anisotropic. For this reason, the more general description of the theory starts from this case. In principle twelve elastic properties are required to relate stresses and strains [5]. These properties are connected, meaning that the number of unknowns required for solving the problem can be reduced to nine non-dependent properties. For a plate of thickness h with two directions of orthotropy along x and y axes, excited by a sound pressure field p , the differential equation describing the lateral vibration w can be written as [6]:

$$D_x \frac{\partial^4 w}{\partial x^4} + 2B \frac{\partial^4 w}{\partial x^2 \partial y^2} + D_y \frac{\partial^4 w}{\partial y^4} + \mu \frac{\partial^2 w}{\partial t^2} = p(x, y, t) \quad (1)$$

where μ is the mass per unit area of the plate, D_j is the bending stiffness per unit width in the j th direction, and B is the effective torsional rigidity of the plate. Such terms are defined as:

$$D_x = \frac{E_x h^3}{12(1 - \nu_x \nu_y)}; \quad D_y = \frac{E_y h^3}{12(1 - \nu_x \nu_y)}; \quad B = \sqrt{D_x D_y} (1 - \sqrt{\nu_x \nu_y}) + \frac{D_x \nu_y + D_y \nu_x}{2} \quad (2)$$

with E_j Young's modulus and ν_j Poisson's ratio in the j th direction. The equation can be simplified since $D_x \nu_y = D_y \nu_x$ and, consequently, $B = \sqrt{D_x D_y}$. The resulting governing differential equation is therefore

$$D_x \frac{\partial^4 w}{\partial x^4} + 2\sqrt{D_x D_y} \frac{\partial^4 w}{\partial x^2 \partial y^2} + D_y \frac{\partial^4 w}{\partial y^4} + \mu \frac{\partial^2 w}{\partial t^2} = p(x, y, t) \quad (3)$$

The apparent bending stiffness of an orthotropic plate can be experimentally determined by means of point mobility measurements. This method is particularly suitable to the case of massive or already-mounted partitions [7], from which smaller samples cannot be cut for measurements in sound transmission suites or other simpler procedures [8]. For a rectangular, simply supported orthotropic plate of dimensions L_x and L_y the point mobility is

$$Y(x_j, y_j) = \sum_{mn} \frac{4i\omega \phi_{mn}^2(x_j, y_j)}{L_x L_y \left[(\sqrt{D_x} k_m^2 + \sqrt{D_y} k_n^2)^2 - \mu\omega^2 \right]} \quad (4)$$

The eigenfunctions $\phi_{mn}(x, y)$ and the eigenvalues k_m and k_n are:

$$\phi_{mn}(x, y) = \sin(k_m x) \sin(k_n y); \quad k_m = \frac{m\pi}{L_x}; \quad k_n = \frac{n\pi}{L_y} \quad (5)$$

It can be shown that the space- and frequency-average of the real part of the point mobility is

$$\langle \text{Re}(\bar{Y}) \rangle = \frac{1}{8\mu^{1/2} D_x^{1/4} D_y^{1/4}} = \frac{1}{8\sqrt{\mu D}} \quad (6)$$

where the effective bending stiffness has here been denoted by $D = \sqrt{D_x D_y}$.

To derive the sound radiation ratio of the panel, the critical frequency f_c is the key parameter:

$$f_c = \frac{c^2}{2\pi} \sqrt{\left(\frac{\mu}{D}\right)} \quad (7)$$

where c is the speed of sound in air. The radiated acoustic power is influenced by the mode type, so in principle the sound radiation ratio should be computed for each mode. However, this is not convenient nor practical, thus the averaging formulation initially proposed by Maidanik [9] and later resumed by Leppington et al. [10] is generally used. The results of the two studies are indeed similar, except close to the critical frequency where the latter is more accurate [11].

Defining $q = \sqrt{f_c/f}$, the wavenumber $k = \omega/c$, $L_{min} = \min\{L_x, L_y\}$ and $L_{max} = \max\{L_x, L_y\}$, the sound radiation ratio $\bar{\sigma}_r$ is given for different frequency ranges:

$$\bar{\sigma}_r = \begin{cases} \frac{L_x + L_y}{\pi q k L_x L_y \sqrt{q^2 - 1}} \left[\ln\left(\frac{q+1}{q-1}\right) + \frac{2q}{q^2 - 1} \right], & \text{for } f < f_c \\ \left(\frac{1}{2} - 0.15 \frac{L_{min}}{L_{max}}\right) \sqrt{k L_{min}}, & \text{for } f = f_c \\ \frac{1}{\sqrt{1 - q^2}}, & \text{for } f > f_c \end{cases} \quad (8)$$

with the constraint that the sound radiation ratios below and above the critical frequency cannot be greater than the sound radiation ratio at the critical frequency.

The knowledge of the bending stiffness (constant in case of homogeneous plate, and frequency-dependent in case of sandwich partitions) can therefore be used to perform the estimation of $\bar{\sigma}_r$.

3. Materials and methods

Two types of measurements have been carried out in sound transmission suites: mobility measurements and *STL* measurements. The measurements have been performed at the KTH – MWL facilities in Stockholm. The sound transmission suites used for the tests consists of a reverberant room (source room) coupled with a semi-anechoic room (receiving room). The samples to be tested have been placed in an opening between the two rooms. The instrumentation used to perform the mobility measurements is made up of an FFT analyzer, an impedance hammer and an accelerometer. Mobility is the transfer function between the vibration velocity response and the force excitation, so the analyzer must be able to properly compute cross functions. The type of transducers adopted depends on the mass per unit area of the device under investigation and the frequency range of interest, which is essential to obtain reliable results. This is especially important in the vehicle industry, where a similar technique is used to evaluate the stiffness of the frame, which is known to impact on driving precision and handling [12].

For the measurements in sound transmission suites, an omnidirectional sound source was placed in the source room while a microphone mounted on a rotating boom measured the sound pressure level in this chamber. Sound intensity and vibration velocity measurements were made in the receiving room in order to determine the energy flowing through the partition and its radiation efficiency. The transducers were connected to a Brüel & Kjær PULSE system.

The partitions tested are of two types: a) Glass Reinforced Plastic (GRP) panel with ribs, and b) sandwich panel with 25.4 mm-balsa core, both about 1810 mm × 1010 mm in size. For the GRP panel, obtaining meaningful mobility data is not simple, since the specimen is not homogeneous. This means that some information, such as the mass per unit area and the moment of inertia, depends upon the considered portion of the panel. Consequently, the accelerometers were randomly placed on the surface of the panel in order to determine an average value of the vibration velocity.

As concerns the GRP panel, the nominal data are relative to the small sample tested into the sound transmission suites, consisting of a flat 15 mm-thick portion of GRP and 2 ribs:

- Young’s modulus $E = 14$ GPa
- mass per unit area $\mu = 23$ kg/m²
- moment of inertia $I = 0.8 \cdot 10^{-7}$ m³

The data characterizing the sandwich panel with balsa core have been determined from the specimen tested at KTH and from literature data. They are listed in the following Table 1.

Table 1: Characteristics of the sandwich specimen layers (m.u. = measurement unit; n.a. = not available).

Quantity	Symbol	m.u.	Laminates	Core
Thickness	h	m	0.0015	0.0225
Density	ρ	kg/m ³	2700	200
Young’s modulus	E	GPa	70	3.7
Shear modulus	G	GPa	n.a.	0.12

4. Results

The determination of the sound transmission loss of the panels have been performed with reference to the EN ISO 15186-1 standard. The *STL*, expressed in one-third octave bands, is calculated as

$$STL = \bar{L}_{p1} - \bar{L}_{In} - 6 \tag{9}$$

where \bar{L}_{p1} is the space-averaged sound pressure level in the source room, measured by a rotating microphone, and \bar{L}_{In} is the average sound intensity level over the panel surface measured in the receiving room by using the scan method outlined in the ISO 9614-2 standard.

The samples (Fig. 1) have been mounted in the opening between the anechoic and the reverberation room, taking care to seal the edges using high-density silicone and, in some cases, adding foil tape to further improve the insulation. The acoustic excitation has been applied in the reverberation room and the intensity measurement has been performed in the anechoic room. The measured *STL* in one-third octave band is shown in Fig. 2 for both the specimen types.

It can be noted that while for the sandwich panel with balsa core the coincidence region can be clearly recognized at a frequency of 500 Hz, the *STL* graph for the ribbed GRP presents two distinct minima, the first one at a frequency of about 200-250 Hz and the second one at a frequency of 1000-1250 Hz. Such behavior, probably due to the different coincidence frequencies of the GRP panel and of the ribs, will be further investigated in the following sections.

During the *STL* measurements, some additional quantities have been determined. In particular, while the noise source was generating a pink noise in the reverberant room, vibration velocity measurements have been performed at 16 positions randomly placed on the surface of the two panels. For each panel it was then possible to compute the average vibration velocity in 1/3 octave bands, as depicted in Fig. 3 together with the average sound intensity flowing through the panels and measured in the receiving room.

A further investigation has been carried out on the panels while mounted in the test opening for the determination of the apparent bending stiffness through point mobility measurements. The results of such tests are given in [13] and will be used to compare the sound radiation efficiency measured in the test rooms according to Leppington’s theory.

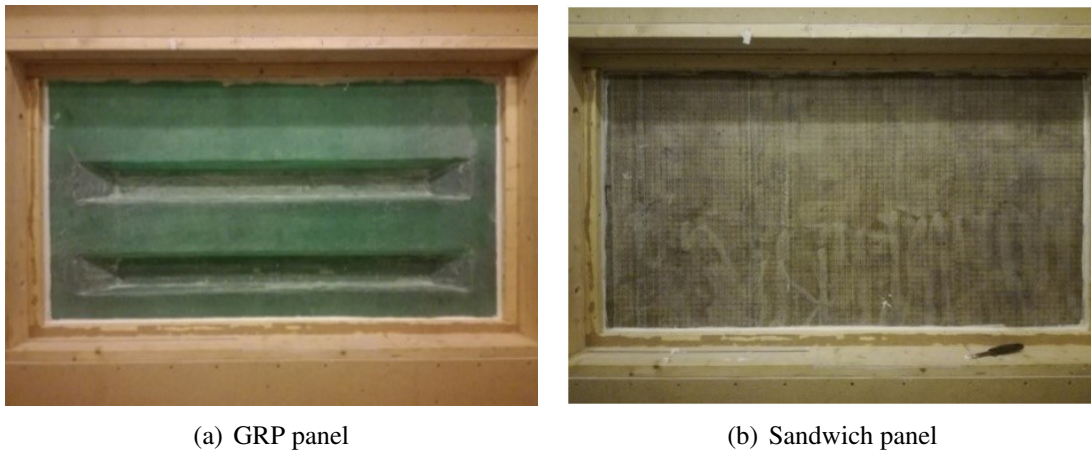


Figure 1: Pictures of the panels mounted in the sound transmission suites.

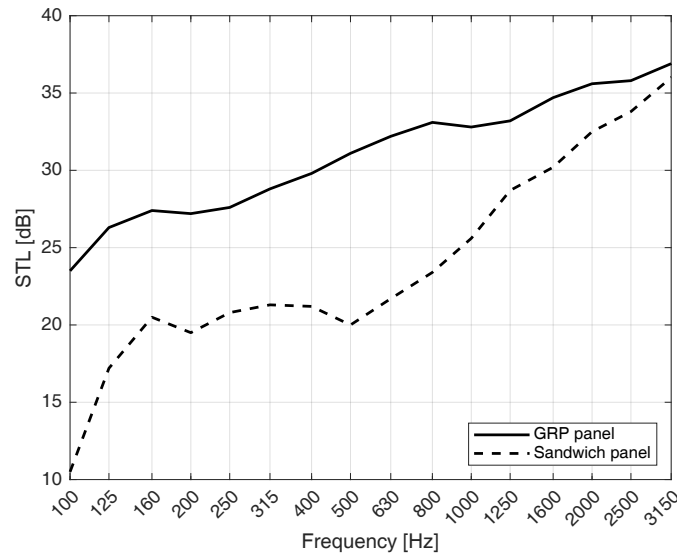


Figure 2: *STLs* of GRP panel (solid line) and sandwich panel (dashed line) measured in sound transmission suites.

5. Sound radiation efficiency and sound radiation index

Sound radiation efficiency is a measurement of the effectiveness of a vibrating surface in generating sound power, which may be a desirable quality (for example, in musical instruments [14]) or a critical aspect to monitor.

The sound radiation index can be determined by measurements of sound pressure level and velocity level, but in this case a correction must be applied which depends on the diffuseness of the sound field [15]. However, the sound radiation index can also be directly calculated from the sound intensity level and vibration velocity level measured in an anechoic room, as:

$$L_{\sigma} = 10 \log_{10} \bar{\sigma}_r = L_I - L_v + 34 \quad (10)$$

The sound radiation index calculated with Eq. 10 as a function of frequency and the values obtained

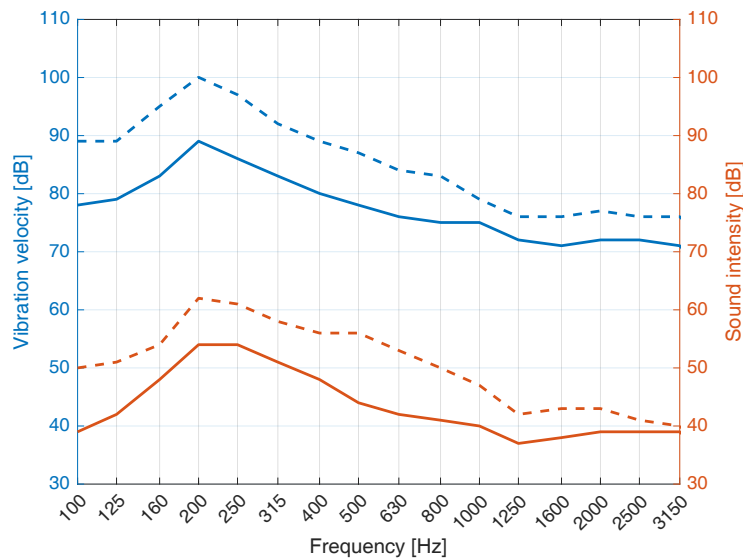


Figure 3: Average vibration velocities and sound intensities measured in the receiving room for the GRP (solid lines) and sandwich (dashed lines) panels.

from point mobility measurements, Eqs. 6-8, are compared for the GRP ribbed panel and for the sandwich with balsa core panel in Fig. 4 and Fig. 5, respectively.

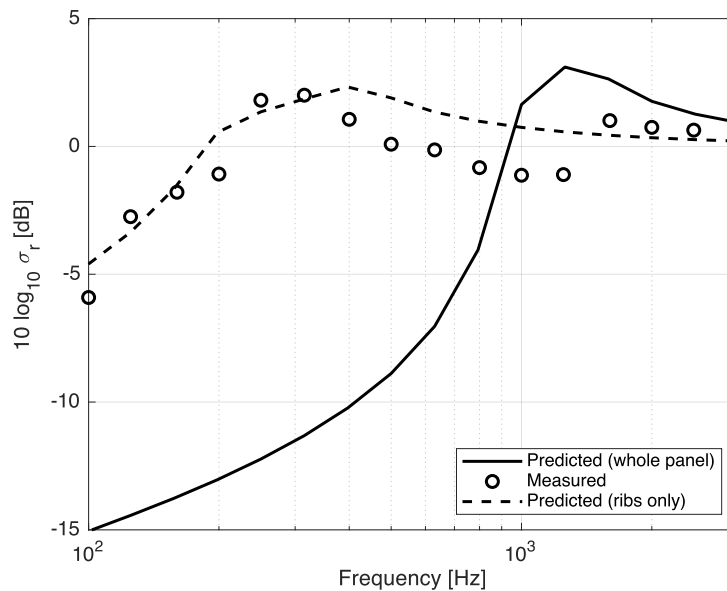


Figure 4: Sound radiation index for the ribbed GRP panel.

As concerns the sound radiation index of the ribbed GRP panel, the values are negative for frequencies well below 250 Hz, which is arguably the coincidence frequency of the ribs. Above 250 Hz the radiation index is very close to 0 while at 1600 Hz the graph has a second maximum due to the coincidence effect in the homogeneous panel. Above 2.5 kHz, the radiation index increases approaching 2 dB. This effect is probably due to the sum of the radiation efficiency of the flat part of the panel and of the ribs. Such behavior is clearly visible also in the sound transmission loss graph of Fig. 2, where the ribbed GRP panel

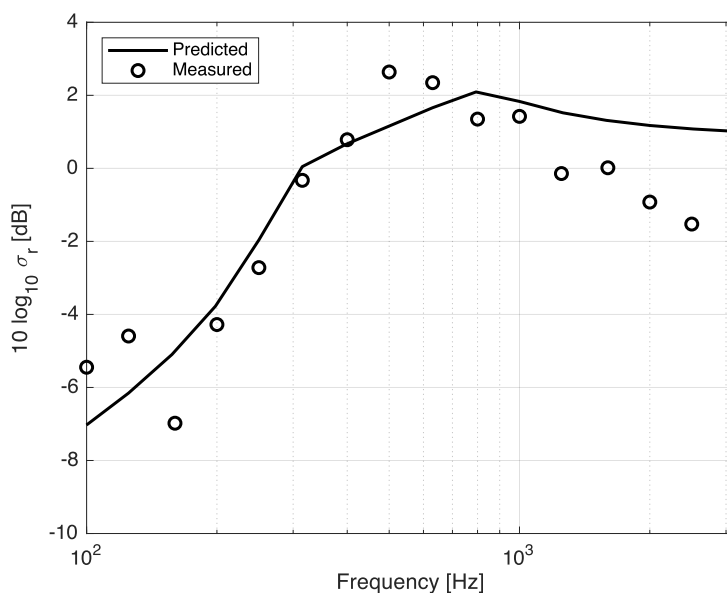


Figure 5: Sound radiation index for the sandwich panel.

tends to have sound insulation characteristics close to the ones of the sandwich panel with balsa core for frequencies above 2 kHz.

As concerns the sandwich panel with balsa core, according to the theory, the radiation index is negative for frequencies below the coincidence region (centered at 500 Hz), and it reaches a maximum of 3 dB at the critical frequency. This behavior is confirmed by experimental measurements. Above 1000 Hz, the sound radiation index becomes negative. The reason is probably that, especially for a thick sandwich structure, the wave motion at high frequencies becomes more complex and other types of waves, like shear waves and anti-phase waves, start to have a significant effect.

6. Conclusions

The sound transmission loss and the sound radiation ratio of composite and sandwich panels can be predicted using classical theories developed for homogeneous panels by using a frequency-dependent “apparent” bending stiffness function instead of a constant value. In this work, the apparent bending stiffness of the structure has been determined by means of space- and frequency-averages of point mobility measurements over two specimens: a glass-reinforced plastic panel and a sandwich panel with balsa core. The resulting sound radiation ratios as a function of frequency have been compared to the values obtained from experimental measurements of vibration velocity and intensity in sound transmission suites. The comparison shows that, for the glass reinforced plastic specimen, the average approach of the point mobility measurements cannot capture correctly the distinct coincidence effects of the panel and the ribs. In this situation, two different analyses should be made. The method provides better results with the sandwich material, where the agreement is good up to the coincidence region. Overall, point mobility measurements proved to be a powerful tool to catch non trivial information about the vibro-acoustic behavior of unconventional structures.

REFERENCES

1. Piana, E. A. and Marchesini, A. How to lower the noise level in the owner's cabin of a yacht through the improvement of bulkhead and floor, *Proceedings of the 21st International Congress on Sound and Vibration*, Beijing, China, 13–17 July, vol. 5, pp. 3692–3699, (2014).
2. Schenone, C., Pittaluga, I., Borelli, D., Kamali, W. and El Moghrabi, Y. The impact of environmental noise generated from ports: Outcome of MESP project, *Noise Mapping*, **3** (1), 26–36, (2016).
3. Di Bella, A. and Remigi, F. Prediction of noise of moored ships, *Proceedings of Meetings on Acoustics*, Montréal, Canada, 2–7 June, vol. 19, (2013).
4. Piana, E. A., Petrogalli, C., Paderno, D. and Carlsson, U. Application of the wave propagation approach to sandwich structures: Vibro-acoustic properties of aluminum honeycomb materials, *Applied Sciences*, **8** (1), (2018).
5. Piana, E. A. and Nilsson, A. C. Sound radiation efficiency of honeycomb and sandwich plates, *Proceedings of the 21st International Congress on Sound and Vibration*, Beijing, China, 13–17 July, vol. 2, pp. 1502–1509, (2014).
6. Nilsson, A. and Liu, B., *Vibro-Acoustics, Volume 1*, Springer-Verlag, Berlin Heidelberg, 2nd edn. (2015).
7. Piana, E. A., Petrogalli, C. and Solazzi, L. Dynamic and acoustic properties of a joisted floor, Obaidat, M., Merkurjev, Y. and Oren, T. (Eds.), *Proceedings of the 6th International Conference on Simulation and Modeling Methodologies, Technologies and Applications, SIMULTECH 2016*, Lisbon, Portugal, 29–31 July, pp. 277–282, (2016).
8. Piana, E. A. and Nilsson, A. C. Prediction of the sound transmission loss of sandwich structures based on a simple test procedure, *Proceedings of the 17th International Congress on Sound and Vibration*, Cairo, Egypt, 18–22 July, vol. 1, pp. 109–116, (2010).
9. Maidanik, G. Response of Ribbed Panels to Reverberant Acoustic Fields, *Journal of the Acoustical Society of America*, **34** (6), 809–826, (1962).
10. Leppington, F. G., Broadbent, E. G. and Heron, K. H. The Acoustic Radiation Efficiency of Rectangular Panels, *Proceedings of the Royal Society of London. Series A, Mathematical and Physical Sciences*, **382** (1783), 245–271, (1982).
11. Nilsson, A. and Liu, B., *Vibro-Acoustics, Volume 2*, Springer-Verlag, Berlin Heidelberg, 2nd edn. (2016).
12. Uberti, S. and Gadola, M. Design of a new high-end street bike, *11th International Design Conference, DESIGN 2010*, Dubrovnik, Croatia, May, pp. 1741–1752, (2010).
13. Piana, E. A., Carlsson, U. and Feng, L. Determination and optimisation of the sound reduction index of ship bulkheads through the wave propagation approach, *Proceedings of ISMA 2018 - International Conference on Noise and Vibration Engineering and USD 2018 - International Conference on Uncertainty in Structural Dynamics*, Leuven, Belgium, 17–19 September, pp. 4527–4541, (2018).
14. Tronchin, L. Modal analysis and intensity of acoustic radiation of the kettledrum, *Journal of the Acoustical Society of America*, **117** (2), 926–933, (2005).
15. Piana, E. A., Marchesini, A. and Nilsson, A. C. Evaluation of different methods to predict the transmission loss of sandwich panels, *Proceedings of the 20th International Congress on Sound and Vibration*, Bangkok, Thailand, 7–11 July, vol. 4, pp. 3552–3559, (2013).